Clim. Past, 13, 1473–1489, 2017
https://doi.org/10.5194/cp-13-1473-2017

Climate of the Past
Open Access

Central Arctic Ocean paleoceanography from ∼ 50 ka to present, on the basis of ostracode faunal assemblages from the SWERUS 2014 expedition

Laura Gemery[1], **Thomas M. Cronin**[1], **Robert K. Poirier**[1,2], **Christof Pearce**[3,4], **Natalia Barrientos**[3], **Matt O'Regan**[3], **Carina Johansson**[3], **Andrey Koshurnikov**[5,6], and **Martin Jakobsson**[3]

[1]U.S. Geological Survey, Reston, Virginia, USA
[2]Rensselaer Polytechnic Institute, Department of Earth & Environmental Sciences, Troy, New York, USA
[3]Department of Geological Sciences and Bolin Centre for Climate Research, Stockholm University, 10691 Stockholm, Sweden
[4]Department of Geoscience, Aarhus University, 8000 Aarhus, Denmark
[5]Tomsk National Research Polytechnic University, Tomsk, Russia
[6]Department of Geophysics, Moscow State University, Moscow, Russian Federation

Correspondence to: Laura Gemery (lgemery@usgs.gov)

Received: 21 February 2017 – Discussion started: 28 March 2017
Revised: 11 August 2017 – Accepted: 28 August 2017 – Published: 3 November 2017

Abstract. Late Quaternary paleoceanographic changes at the Lomonosov Ridge, central Arctic Ocean, were reconstructed from a multicore and gravity core recovered during the 2014 SWERUS-C3 Expedition. Ostracode assemblages dated by accelerator mass spectrometry (AMS) indicate changing sea-ice conditions and warm Atlantic Water (AW) inflow to the Arctic Ocean from ∼ 50 ka to present. Key taxa used as environmental indicators include *Acetabulastoma arcticum* (perennial sea ice), *Polycope* spp. (variable sea-ice margins, high surface productivity), *Krithe hunti* (Arctic Ocean deep water), and *Rabilimis mirabilis* (water mass change/AW inflow). Results indicate periodic seasonally sea-ice-free conditions during Marine Isotope Stage (MIS) 3 (∼ 57–29 ka), rapid deglacial changes in water mass conditions (15–11 ka), seasonally sea-ice-free conditions during the early Holocene (∼ 10–7 ka) and perennial sea ice during the late Holocene. Comparisons with faunal records from other cores from the Mendeleev and Lomonosov ridges suggest generally similar patterns, although sea-ice cover during the Last Glacial Maximum may have been less extensive at the new Lomonosov Ridge core site (∼ 85.15° N, 152° E) than farther north and towards Greenland. The new data provide evidence for abrupt, large-scale shifts in ostracode species depth and geographical distributions during rapid climatic transitions.

1 Introduction

Environmental conditions are changing rapidly in the Arctic Ocean today, but a longer time perspective is necessary to assess and contextualize these changes and their contributing factors. These changing conditions include sea-ice extent and thickness (Stroeve et al., 2012, 2014; Laxon et al., 2013), as well as ocean temperature, stratification, circulation, chemistry, and ecology (Polyakov et al., 2017; Moore et al., 2015; Chierici and Fransson, 2009; Rabe et al., 2011; Grebmeier et al., 2006; Grebmeier, 2012; Wassmann et al., 2011). Sea-ice extent and thickness, in particular, are challenging parameters to reconstruct because most sea-ice proxies lack temporal and geographical resolution (Stein et al., 2012). Sea-ice extent and thickness, however, are very important variables because they influence albedo, near-surface salinity, light levels, surface-to-seafloor organic carbon flux, and other variables that are important to ecosystems. In fact, sea ice exerts a primary control on Arctic biological and geochemical cycles (Anderson et al., 2011), and sea-ice changes are in part responsible for fast-feedback climate changes during the geologic past (Polyak et al., 2010).

Before the last few decades, instrumental oceanographic records were relatively sparse, and sediment proxy records provided insight into past sea-ice conditions and ocean circulation changes from all regions of the Arctic. These records are especially important for examining sea-ice history during past climate changes before the availability of instrumental records. The composition and abundance of marine microfossils preserved in many Arctic sediments provide an important constituent that help address the growth and decay of ice sheets. For example, several excursions in records of oxygen and carbon isotopes of planktic foraminifers from Arctic sediment cores have been interpreted as releases of freshwater from collapsing continental ice sheets during glaciations and glacial terminations (Stein et al., 1994; Nørgaard-Pedersen et al., 1998).

This paper examines temporal changes in microfossil shells from ostracode indicator species that shed light on biological productivity and sea-ice extent during the last ~ 50 kyr, including Marine Isotope Stage (MIS) 3, the Last Glacial Maximum (LGM, ~ 21 ka), the deglacial interval and the Holocene. Ostracoda are bivalved crustaceans that inhabit Arctic marine habitats and whose assemblages (i.e., Cronin et al., 1994, 1995; Poirier et al., 2012) and shell chemistry (i.e., Cronin et al., 2012) have been used extensively as proxies to reconstruct Arctic paleoceanography and sea-ice history (i.e., Cronin et al., 2010). Most ostracode species are benthic in habitat and their ecology reflects bottom water environmental conditions. Benthic ecosystems rely on biological productivity in the upper water column, and so benthic biomass production and community structure also reflect sea-ice cover and surface-to-bottom ecosystem links (Grebmeier and Barry, 1991; Grebmeier et al., 2006). However, two pelagic/epipelagic ostracode taxa are used in this paper to indicate water mass conditions.

Sediment cores for this study were collected during the 2014 SWERUS-C3 (Swedish – Russian – US Arctic Ocean Investigation of Climate-Cryosphere-Carbon Interactions) Leg 2 expedition from previously unstudied regions of the Siberian margin and the Lomonosov Ridge. The radiocarbon-dated records presented here are from 85.15° N, 152° E on the Lomonosov Ridge in the central Arctic Ocean, a site located at ~ 800 m near the transition between Atlantic Water and Arctic Intermediate Water in the modern Arctic Ocean. During prior glacial–interglacial cycles, the region was influenced to various degrees by the strength and depth penetration of Atlantic Water. For example, during glacial intervals when thick ice shelves covered much of the Arctic Ocean (Jakobsson et al., 2016), Arctic Intermediate Water warmed (Cronin et al., 2012) and likely entrained to greater water depths (Poirier et al., 2012). Consequently, the new results, when compared to published faunal records from other regions of the Arctic Ocean (Fig. 1a, Table 1), show some regional differences but an overall remarkable consistency in central Arctic faunal abundance changes during the late Quaternary.

2 Arctic oceanography

The Arctic Ocean is strongly stratified, with distinct water masses separated by vertical changes in salinity and temperature (Fig. 1b). The following summary of Arctic water masses and circulation is taken from Aagaard and Carmack (1989), Anderson et al. (1994), Jones (2001), Olsson and Anderson (1997) and Rudels et al. (2012, 2013). Arctic Ocean water masses include a fresh, cold Polar Surface Water layer (PSW; $T = \sim 0$ to -2 °C, $S = \sim 32$ to 34), found between ~ 0 and 50 m. The PSW is characterized by perennial ice in most regions and seasonal sea ice in the margins of the Arctic Ocean. Beneath the sea-ice cover, a strong halocline separates the PSW from the underlying warmer, denser water mass of North Atlantic origin (Atlantic Water, AW; ~ 200 to 1000 m, $T = >0$ °C, $S = \sim 34.6$ to 34.8). One branch of the AW flows into the Arctic Ocean from the Nordic seas along the eastern Fram Strait off the west coast of Spitsbergen and another branch flows through the Barents Sea. An intermediate-depth water mass below the AW in the Eurasian Basin at ~ 1000–1500 m is called the Arctic Intermediate Water (AIW; $T = -0.5$ to 0 °C, $S = \sim 34.6$ to 34.8). Below 2000 m, the deep Arctic basins are filled with Arctic Ocean Deep Water (AODW; $T = -1.0$ to -0.6 °C, $S = 34.9$; Somavilla et al., 2013). Bathymetry is a dominant factor governing circulation patterns for AW and AIW, and a sharp front over the Lomonosov Ridge near the SWERUS-C3 core site studied here partially isolates these waters in the Eurasian Basin from the Canadian Basin (Fig. 1b).

In addition to Arctic Ocean stratification, other factors influence sea-ice decay and growth over geologic time (i.e., Polyak et al., 2010). A recent study by Stein et al. (2017) notes the importance of large-scale atmospheric circulation patterns, such as the North Atlantic Oscillation (NAO) and Arctic Oscillation (AO), and radiative forcing (i.e., solar activity) on Holocene sea-ice thickness, extent and duration. The NAO and AO influence changes of the relative position and strength of the two primary Arctic Ocean surface-current systems, the Beaufort Gyre in the Amerasian Basin and the Transpolar Drift in the Eurasian Basin (Fig. 1a; Rigor et al., 2002; Stroeve et al., 2014). Data resulting from the SWERUS expedition will help improve understanding of the spatial patterns of sea-ice and intermediate depth circulation, given the extreme variability in sea ice in this region recently evident from satellite records (Serreze and Stroeve, 2015; Stroeve et al., 2014), the importance of the Transpolar Drift in sea-ice export through Fram Strait (Polyak et al., 2010; Smedsrud et al., 2017) and new evidence for the influence of inflowing Atlantic Water on sea ice and "Atlantification" of the Eurasian Basin (Polyakov et al. 2017).

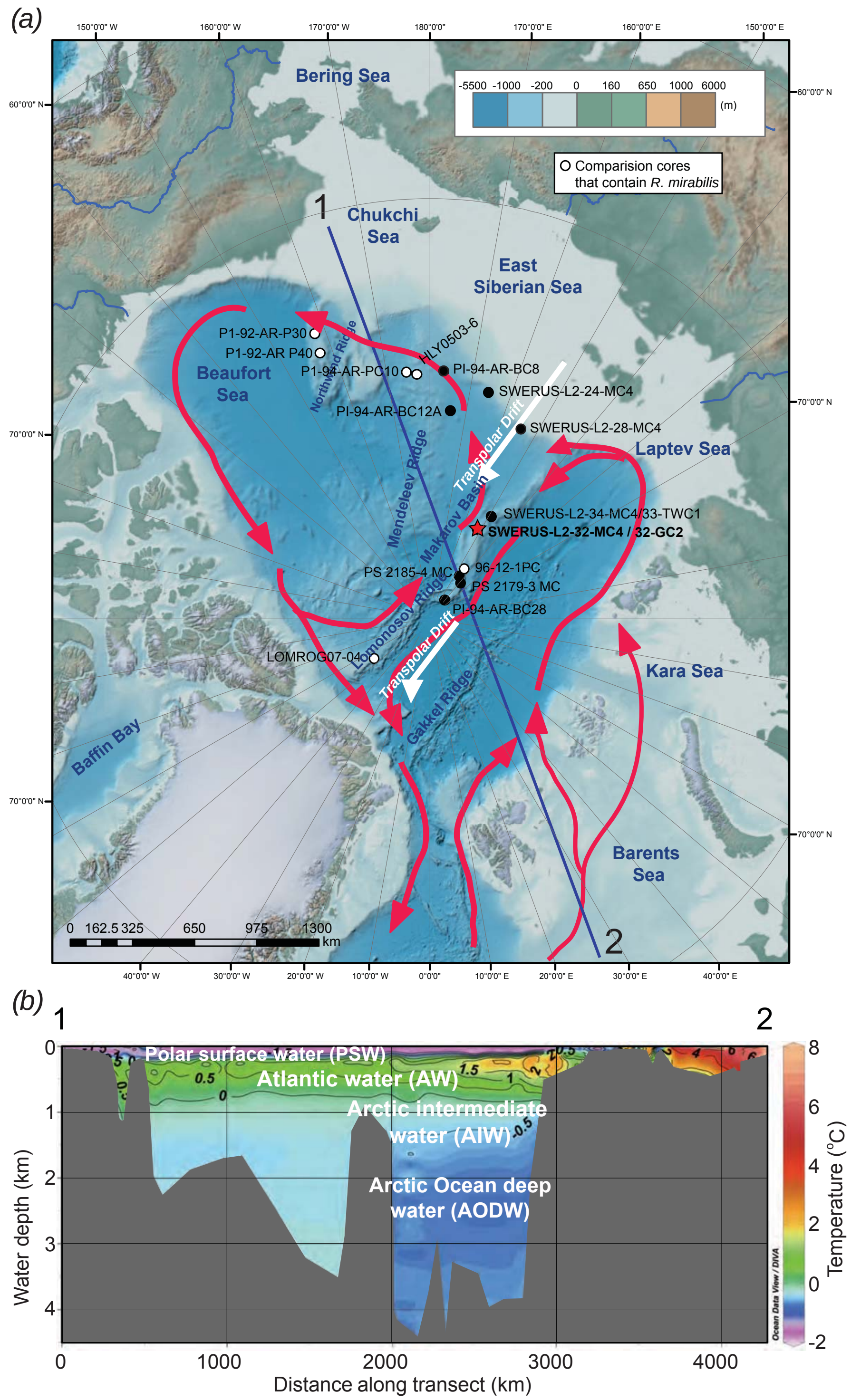

Figure 1. **(a)** International Bathymetric Chart of the Arctic Ocean showing the location of this study's primary sediment cores on the Lomonosov Ridge (red star: 32-GC2 and 32-MC4), as well as other core sites discussed in this paper (black and white circles). (See Table 1 for supplemental core data.) White circles designate cores that contain *Rabilimis mirabilis* events. Red arrows show generalized circulation patterns of warm Atlantic Water in the Arctic Ocean. White arrows indicate the surface flow of the Transpolar Drift, which moves sea ice from the Siberian coast of Russia across the Arctic Basin, exiting into the North Atlantic off the east coast of Greenland. Transect line through the map from "1" in the Chukchi Sea to "2" in the Barents Sea shows direction of temperature profile in **(b)**. **(b)** Cross section of modern Arctic Ocean temperature profile from showing major water masses. PSW: Polar Surface Water; AL: Atlantic layer; AIW: Arctic Intermediate Water; AODW: Arctic Ocean Deep Water. Ocean Data View source: Schlitzer, 2012. Ocean Data View: http//odv.awi.de.

Table 1. Expedition and core site data for cores presented in this study.

Year	Expedition	Core name	Latitude	Longitude	Water depth (m)	Location
2014	SWERUS-L2	SWERUS-L2-32-MC4	85.14	151.59	837	Lomonosov Ridge
2014	SWERUS-L2	SWERUS-L2-32-GC2	85.15	151.66	828	Lomonosov Ridge
2014	SWERUS-L2	SWERUS-L2-24-MC4	78.80	165.38	982	E. Siberian Sea Slope
2014	SWERUS-L2	SWERUS-L2-28-MC1	79.92	154.35	1145	E. Siberian Sea Slope
2014	SWERUS-L2	SWERUS-L2-33-TWC1	84.28	148.65	888	Lomonosov Ridge
2014	SWERUS-L2	SWERUS-L2-34-MC4	84.28	148.71	886	Lomonosov Ridge
1994	AOS SR96-1994	PI-94-AR-BC28	88.87	140.18	1990	Lomonosov Ridge
1991	Arctic 91	PS 2179-3 MC	87.75	138.16	1228	Lomonosov Ridge
1991	Arctic 91	PS 2185-4 MC	87.53	144.48	1051	Lomonosov Ridge
1994	AOS SR96-1994	PI-94-AR-BC8	78.13	176.75	1031	Mendeleev Ridge
1994	AOS SR96-1994	PI-94-AR-BC12A	79.99	174.29	1683	Mendeleev Ridge
2005	HOTRAX	HLY0503-6	78.29	−176.99	800	Mendeleev Ridge
1994	AOS SR96-1994	P1-94-AR-PC10	78.15	−174.63	1673	Mendeleev Ridge
1992	USGS-Polar Star	P1-92-AR P40	76.26	−157.55	700	Northwind Ridge
1992	USGS-Polar Star	P1-92-AR-P30	75.31	−158.05	765	Northwind Ridge
2007	LOMROG 07	LOMROG07-PC-04	86.70	−53.77	811	Lomonosov Ridge
1996	Oden 96	96-12-1PC	87.10	144.77	1003	Lomonosov Ridge

3 Materials and methods

3.1 Core material and sample processing

Cores for this study were obtained during the September 2014 SWERUS-C3 (Leg 2) expedition to the eastern Arctic Ocean aboard Swedish Icebreaker *Oden*. Figure 1 shows the location of multicore SWERUS-L2-32-MC4 (85.14° N, 151.57° E; 837 m) and nearby gravity core SWERUS-L2-32-GC2 (85.15° N; 151.66° E, 828 m) on the Lomonosov Ridge. These cores are hereafter referred to as 32-MC and 32-GC, respectively. Both cores were stored at 4 °C and sampled at the Department of Geological Sciences, Stockholm University. Processing of the samples involved washing the sediment with water through a 63 µm mesh sieve. Core 32-MC was processed in Stockholm, while 32-GC was processed at the U.S. Geological Survey (USGS) laboratory in Reston, Virginia. Sediment samples (1 cm thick, ∼ 30 g prior to processing) were taken every centimeter in 32-MC along its 32 cm length. Section 1 (117 cm) of 32-GC was sampled every 2–3 cm (2 cm thick, ∼ 45–60 g wet weight).

After processing and oven-drying the samples, the residual > 125 µm size fraction was sprinkled on a picking tray and ostracodes were removed to a slide. One exception for expediency is that specimens of the genus *Polycope* were counted and not removed from the sediment. A total of ∼ 300 specimens were studied from each sample of 32-MC. More detailed counts of some samples in 32-MC were done periodically, where all specimens were picked and/or counted to ensure that 300 specimens provided a representative assemblage. In 32-GC, all specimens were picked and/or counted in each sample. Ostracodes were present throughout the entire studied intervals of both 32-MC and down to 62 cm in 32-GC. Planktic and benthic foraminifers were also present in abundance but not studied.

3.2 Chronology, reservoir corrections and sedimentation

Nine radiocarbon (^{14}C) ages were obtained from core 32-MC using accelerator mass spectrometry (AMS) (Fig. 2, Table 2). Most dates were obtained on mollusks (*Nuculidae* and *Arcidae* spp.), except a few samples where mollusks and benthic foraminifera were combined. Two ages from 32-GC were obtained using a combination of mollusks, foraminifera and ostracode shells. The final age models representing the two cores combined are based on all the calibrated ^{14}C ages listed in Table 2. Generally, ages > 40 ka should be considered with caution because of large uncertainties in the radiocarbon calibration curve and high sensitivity to even extremely small levels of contamination. Calibration into calendar years was carried out using Oxcal4.2 (Bronk Ramsey, 2009) and the Marine13 calibration curve (Reimer et al., 2013), using a local marine reservoir correction, ΔR, of 300 ± 100 years. Because ΔR values for the central Arctic Ocean were not constant during the last 50 kyr, it is difficult to date pre-Holocene sediments independently (Pearce et al., 2017; Hanslik et al., 2010), and improved age models may be available in the future.

Patterns in ostracode assemblages in both cores were used to correlate cores 32-MC and 32-GC and produce a composite faunal record, which led to a 3 cm offset for core 32-GC. After adding the 3 cm offset to sample depths of 32-GC, the 32-MC core chronology was applied down to 31.5 cm core depth (dated at 39.6 ka). The average sedimentation rate at the core site was ∼ 1.5 cm kyr^{-1}, which is typical of central Arctic Ocean ridges (Backman et al., 2004; Polyak et al., 2009).

Table 2. Radiocarbon dates for SWERUS 32 cores, uncalibrated ^{14}C age and calibrated ^{14}C chronology. All ages as calibrated years BP. $\Delta R = 300 \pm 100$ years (Reimer and Reimer, 2001). Marine13 calibration curve (Reimer et al., 2013).

32-MC/GC chronology		Unmodeled 2σ (2 SD)				Modeled 2σ (2 SD)			
Lab number (^{14}C date age, error)	Depth (cm)	From	To	Mean	Error	From	To	Mean**	Error
OS-124799 (3410, 25)	2.5	3168	2698	2912	124	3045	2605	2802	105
OS-124798 (6110, 20)	4.5	6435	5974	6213	116	6317	5902	6140	113
OS-124599 (7920, 35)	5.5	8313	7874	8085	110	8176	7766	7972	101
OS-124598 (8290, 30)	8.5	8715	8207	8465	119	8576	8187	8385	99
OS-124597 (11 000, 35)	11.5	12 525	11 661	12 094	222	12 191	11 353	11 831	230
OS-124754 (11 200, 40)	14.5	12 635	12 040	12 365	164	12 625	12 008	12 381	165
OS-125185 (18 650, 80)	19.5	22 116	21 357	21 729	183	21 973	21 252	21 637	179
OS-125190 (29 400, 280)	24.5	33 567	31 805	32 733	462	33 298	31 585	32 423	455
OS-125192 (35 400, 560)	31.5	40 705	38 099	39 301	638	40 858	38 451	39 608	608
OS-127484 (40 000, 1700)	33*	47 589	40 881	43 837	1646	44 472	40 403	42 428	1002

* Sample collected from 32-GC; original depth was 36 cm but corrected by 3 cm based on ostracode correlation with 32-MC.
** We used the modeled, mean, 2σ age to plot species' relative frequencies.

The lower section of 32-GC, from 31.5 to 61 cm, is beyond the limit of radiocarbon dating. However, the lithostratigraphy of the gravity core can be readily correlated to other records from the central Lomonosov Ridge, where multiple dating techniques constrain the approximate positions of MIS 4 and 5 boundaries (Jakobsson et al., 2001; O'Regan, 2011). A correlation between SWERUS-C3 32-GC and AO96/12-1PC was previously presented in Jakobsson et al. (2016). The correlation is supported by the occurrences in 32-GC of the calcareous nannofossil *E. huxleyi* (Fig. 2). Based on this longer-term correlation, sediments between 31 and 61 cm are less than 50 ka. This age estimate is consistent with previous work on the Lomonosov Ridge, revealing a prominent transition from coarse-grained, microfossil-poor sediments (diamict) into bioturbated, finer-grained, microfossiliferous sediments that occurred during MIS 3 at approximately 50 ka (Spielhagen et al., 2004; Nørgaard-Pederson et al., 2007).

4 Results and discussion

4.1 Ostracode taxonomy and ecology

The SWERUS 32 cores contained a total of 13 767 ostracode specimens in 32-MC and a total of 5330 specimens in the uppermost 5–62 cm of 32-GC (the top few centimeters below the seafloor were not recovered in the gravity core). The bottom 54 cm of 32-GC (section 1 from 63 to 117 cm) was barren of calcareous material. Twenty-eight ostracode species were identified in 32-MC and 21 species were identified in 32-GC. Supplement Tables S1 and S2 provide all species and genus census data for 32-MC and 32-GC, respectively. Data will also be accessible at NOAA's National Centers for Environmental Information (NCEI, https://www.ncdc.noaa.gov/paleo-search/). The primary sources of taxonomy and ecology were papers by Cronin et al. (1994, 1995, 2010), Gemery et al. (2015), Joy and Clark (1977), Stepanova (2006), Stepanova et al. (2003, 2007, 2010), Whatley et al. (1996, 1998), and Yasuhara et al. (2014).

Podocopid ostracodes were identified at the species level except the genera *Cytheropteron* and myodocopid *Polycope*. Table 3 provides a list of species included in the genus-level groups, which was sufficient to reconstruct paleoenvironmental changes. There are several species of *Cytheropteron* in the deep Arctic Ocean, but they are not ideal indicator species given their widespread modern distributions. There are at least eight species of *Polycope* in the Arctic Ocean, but juvenile molts of *Polycope* species are difficult to distinguish from one another. Most specimens in 32-MC and 32-GC be-

Table 3. List of species included in genus-level groups.

Group name	Species included in group
Cytheropteron spp.	*Cytheropteron higashikawai* Ishizaki, 1981, *Cytheropteron scoresbyi* Whatley and Eynon, 1996, *Cytheropteron sedovi* Schneider, 1969 and *Cytheropteron parahamatum* Yasuhara, Stepanova, Okahashi, Cronin and Brouwers, 2014.
Polycope spp.	*P. inornata* Joy and Clark, 1977 and *P. bireticulata* Joy and Clark, 1977. (For scanning electron microscope images, see Joy and Clark, 1977: plate 3, fig. 1; Yasuhara et al., 2014: plate 3, figs. 2–5 and plate 2, figs. 1–2.) May include *P. arcys* (Joy and Clark, 1977), *P. punctata* (Sars, 1869), *P. bispinosa* Joy and Clark, 1977, *P. horrida* Joy and Clark, 1977, *P. moenia* Joy and Clark, 1977, *P. semipunctata* Joy and Clark, 1977, *P. orbicularis* Sars, 1866. *P. pseudoinornata* Chavtur, 1983 and *P. reticulata* Muller, 1894

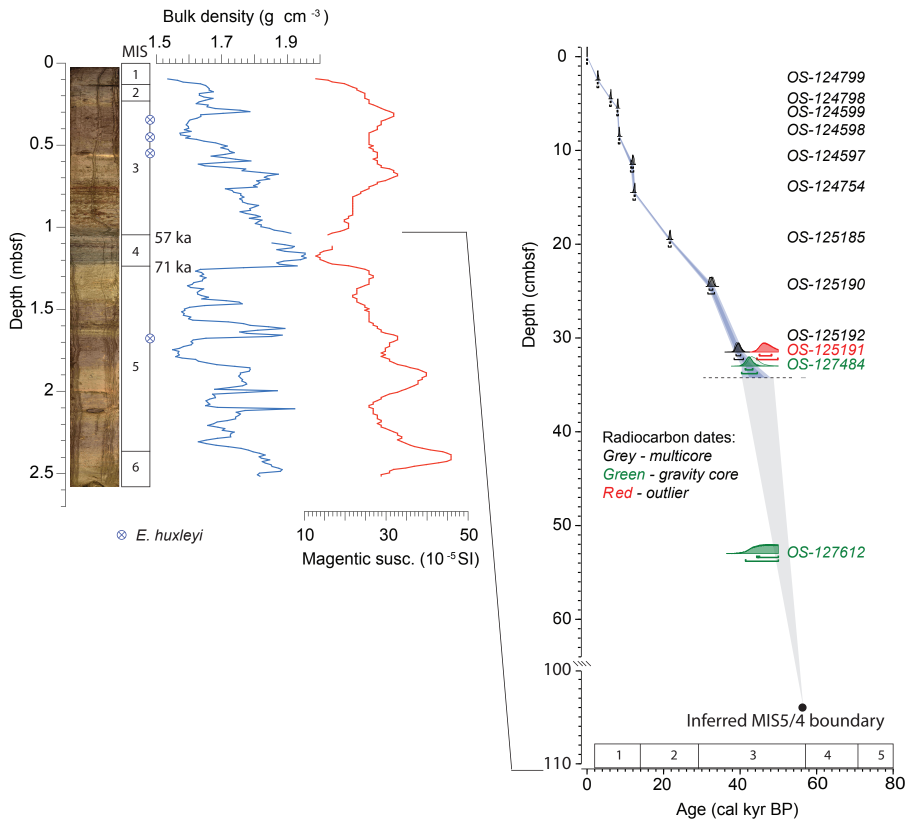

Figure 2. Chronology and stratigraphy of SWERUS-32-GC and 32-MC. Bulk density and magnetic susceptibility profiles for 32GC were previously correlated to the well-dated 96-12-1PC core by Jakobsson et al. (2016). Bulk density primarily reflects changes in grain size, with coarser material having a higher density than finer-grained material. The overall position of MIS 5 is supported by the occurrence of *E. huxleyi*. The chronology for the upper 30–35 cm is based on radiocarbon dating in both 32-MC and 32-GC. Beyond the range of radiocarbon dating, an extrapolation to the inferred position of the MIS 3–4 boundary (57 ka at 105 cm) is applied.

longed to *P. inornata* Joy and Clark, 1977 and *P. bireticulata* Joy and Clark, 1977. Nonetheless, most *Polycope* species co-occur with one another, are opportunistic in their ecological strategy, and dominate assemblages associated with high surface productivity and organic matter flux to the bottom (Table 4; Karanovic and Brandão, 2012, 2016).

The relative frequency (percent abundance) of individual dominant taxa is plotted in Fig. 3 and listed in Supplement

Table 4. Summary of indicator species, pertinent aspects of their modern ecology and paleoenvironmental significance.

Species	Modern ecology/paleoenvironmental significance
Acetabulastoma arcticum (Schornikov, 1970)	The stratigraphic distribution of *A. arcticum* is used as an indicator of periods when the Arctic Ocean experienced thicker sea-ice conditions but not fully glacial conditions when productivity would have halted. This pelagic ostracode is a parasite on *Gammarus* amphipods that live under sea ice in modern, perennially sea-ice-covered regions in the Arctic (Schornikov, 1970). Cronin et al. (2010) used *A. arcticum's* presence in 49 late Quaternary Arctic sediment cores as a proxy to reconstruct the Arctic Ocean's sea-ice history during the last ∼ 45 kyr.
Krithe spp.	Species of the genus *Krithe* typically occur in low-nutrient habitats spanning across a range of cold, interstadial temperatures but are especially characteristic of AODW (Cronin et al., 1994, 1995, 2014). In SWERUS-32 cores, *K. hunti* was far more prevalent than *K. minima.* From a modern depth–distribution analysis using AOD, *K. hunti* appears in greatest abundance (50–80 % of the assemblage) at depths between 2000 to 4400 mwd; however, this taxon is also found in significant numbers (20–50 %) at depths between 400 to 2000 m. With a preference for deeper, cold, well-ventilated depths, *Krithe* spp. events are useful in identifying late Quaternary shifts in Arctic Ocean water masses and making biostratigraphic correlations (Cronin et al., 2014).
Polycope spp.	Today, this Atlantic-derived, myodocopid genus is in highest abundance (40–60 % of assemblage) in cold intermediate-depth waters between 800 and 2300 mwd. It characterizes fine-grained, organic-rich sediment in well-oxygenated water. In fossil assemblages, *Polycope* is indicative of areas with high productivity that are seasonally ice-free or have variable or thin sea-ice cover (Cronin et al., 1995; Poirier et al., 2012).
Cytheropteron spp.	The two dominant *Cytheropteron* species in 32-MC and 32-GC are *C. sedovi* and *C. scoresbyi,* along with lower but significant numbers of *C. parahamatum* (reaches 24 % of assemblage at 10 ka) and *C. higashikawai* (fluctuates in very low numbers between 0 and 3 % at any given time in downcore samples). These particular *Cytheropteron* species are broadly diagnostic of deeper, well-ventilated water masses (AIW and AODW).
Pseudocythere caudata Sars, 1866	This species of North Atlantic origin rarely exceeds > 15 % in modern Arctic Ocean assemblages. It characterizes lower AW and AIW at depths of 1000–2500 mwd. It usually co-occurs with *Polycope* spp. in fossil assemblages and may be associated with surface conditions (Cronin et al., 1994, 1995, 2014), but more work needs to be done on its ecological significance.

Table S3. Abundances were computed by dividing the number of individual species found in each sample by the total number of specimens found. For 32-MC, using the algorithm for a binomial probability distribution provided by Raup (1991), ranges of uncertainty ("error bars") were calculated at the 95 % fractile for the relative frequency in each sample to the relative frequency of each species and the total specimen count of each sample at a given core depth (Supplement Table S4). Faunal densities were high enough to allow comparisons from sample to sample, and Supplement Table S4 lists the density of ostracode specimens per gram of dry sediment, which averaged > 125 shells per gram sediment. For this study of the SWERUS-C3 32 cores, the focus was on an epipelagic species (*Acetabulastoma arcticum)*, a pelagic genus (*Polycope* spp.), three benthic species *(Krithe hunti*, *Pseudocythere caudata*, *Rabilimis mirabilis)* and a benthic genus *(Cytheropteron* spp.). Table 4 provides an overview of pertinent aspects of these species' ecology that have paleoceanographic application.

4.2 Temporal patterns in ostracode indicator species from SWERUS-C3 32-MC/GC

The faunal patterns in cores from the SWERUS-C3 32-MC/GC sites confirm faunal patterns occurring over much of the central Arctic Ocean during the last 50 kyr, including the MIS 3–2 (∼ 50 to 15 ka), the last deglacial interval (∼ 15 to 11 ka), and the Holocene (∼ 11 ka to present). Similar patterns are seen in both the multicore and gravity core. Relative frequencies of indicator taxa in cores 32-MC and 32-GC (Fig. 3) show four distinct assemblages, which are referred to as informal faunal zones following previous studies (Cronin et al., 1995; Poirier et al., 2012). These zones are as follows: (1) *Krithe* zone (primary abundance up to 80 % during ∼ 45–42 ka and a secondary abundance of 5–10 % during ∼ 42–35 ka), (2) *Polycope* zone (with abundance of 50 to 75 % during ∼ 40–12 ka, also containing a double peak in abundance of *P. caudata*), (3) *Cytheropteron–Krithe* zone (12–7 ka), and (4) *Acetabulastoma arcticum* zone (∼ 7 ka–present). This paper briefly discusses the paleoceanographic significance of each period in the following Sects. 4.3–4.5 based on the comparison cores presented in Figs. 4 and 5. Figures 4 and 5 compare the new SWERUS-C3 results from 32-MC with published data from box and multicores from the Lomonosov and Mendeleev ridges, respectively, covering a range of water depths from 700 to 1990 m. Most records extend back to at least 45 ka, and the age model for each core site is based on calibrated radiocarbon ages from that site (i.e., Cronin et al., 2010, 2013; Poirier et al., 2012). In addition, Sect. 4.6 discusses a potential new indicator species, *R. mirabilis*, which exhibits distinct faunal migrations that coincide with *Krithe* zones in 32-MC/GC. *R. mirabilis* lives on today's continental shelf but is found in limited intervals in sediment cores that are far outside its usual depth and geographic range. *R. mirabilis* migrations are documented not only in 32-MC/GC but also in cores 96-12-1PC, HLY0503-06JPC, P1-94-AR-PC10, P1-92-AR-PC40, LOMROG07-04 and P1-92-AR-PC30.

4.3 MIS 3–2 (∼ 50–15 ka)

A strong peak in the abundance of *Krithe hunti* (Fig. 3) is seen in 32-GC sediments estimated to be ∼ 45–42 ka in age. A similar peak of lower but still significant abundance also occurs in sediments dated between 42 and 35 ka, and this peak is consistent with other cores on the Mendeleev Ridge and particularly on the Lomonosov Ridge (Figs. 4, 5). Prior studies of Arctic ostracodes have shown that *Krithe* typically signifies cold well-ventilated deep water and perhaps low food supply (Poirier et al., 2012, and references therein). *Krithe* is also a dominant component (> 30 %) of assemblages in North Atlantic Deep Water (NADW) in the subpolar North Atlantic Ocean. Its abundance varies during glacial–interglacial cycles, reaching maxima during interglacial and interstadial periods (Zarikian et al., 2009). Peaks in the abundance of *Krithe* in the Arctic Ocean probably signify faunal exchange between the North Atlantic Ocean and the Greenland–Norwegian seas through the Denmark Strait and Iceland–Faroe Ridge and the central Arctic through the Fram Strait. In other Arctic Ocean cores, the ostracode genus *Henryhowella* is often associated with *Krithe* sp. in sediments dated between ∼ 50 and 29 ka (MIS 3), and its absence in the 32-MC/GC cores may reflect the relatively shallow depth at the coring site. While *Henryhowella* was absent in records from this site, *R. mirabilis* abruptly appears and spikes to an abundance of 60 % at 40 ka, which coincides with the *Krithe* zone.

A. arcticum is present in low abundance (∼ 5 %) in sediment dated at ∼ 42 to 32 ka in 32-MC/GC (Fig. 3), signifying intermittent perennial sea ice. A second increase in abundance of *A. arcticum* corresponds to a (modeled, mean, 2σ) radiocarbon date of 21.6 ka. This suggests the location of this core may not have been covered by thick ice during the LGM as long as other areas.

A *Krithe* to *Polycope* shift occurred at ∼ 35–30 ka. This "K–P shift" is a well-documented, Arctic-wide transition (Cronin et al., 2014) that has paleoceanographic significance as well as biostratigraphic utility. *Polycope* is clearly the dominant genus group from sediment dated ∼ 40–12 ka in 32-MC/GC and all sites on the Lomonosov and Mendeleev ridges (Figs. 4, 5), signifying high productivity likely due to an intermittent, rapidly oscillating sea-ice edge at the surface. *P. caudata* has varying percentages (3–14 %) in sediment dated ∼ 40–12 ka, depending on the site. *P. caudata* is an indicator of AIW and Cronin et al. (2014) report that it appears to be ecologically linked to the surface conditions. *Cytheropteron* spp. is present in moderate abundance (20–30 %) in sediment dated ∼ 35–15 ka.

Overall, the faunal characteristics from this time period imply relatively restricted and/or poorly ventilated intermediate waters near the 32-MC/GC site. The major exception to this corresponds with the pronounced peaks in *Krithe* and *R. mirabilis*. This significant shift in faunal composition implies changes in ice margins, AW inflow, deep-ocean ventilation and/or enhanced deep-water transfer between the central Arctic Ocean and the North Atlantic.

4.4 The last deglacial interval (∼ 15 to 11 ka)

The major shift from *Polycope*-dominated to *Cytheropteron-Krithe*-dominated assemblages occurs in sediment dated 12 ka in 32-MC/GC and ∼ 15–12 ka in other Lomonosov and Mendeleev Ridge cores. In 32-MC/GC, *Krithe* reappears in low (10 %) but significant abundance after 11 ka after being absent during MIS 2. Both *Cytheropteron* and *Krithe* are typical faunas in NADW. Although low sedimentation rates prevent precise dating of this shift, it almost certainly began ∼ 14.5 ka at the Bølling–Allerød warming transition. Because the Bering Strait had not opened yet (Jakobsson et al., 2017), this faunal shift must have been related to one or several of the following changes: (1) atmospheric warming, (2) strong Atlantic Water inflow through the Barents Sea, and (3) strong Atlantic Water inflow through the eastern Fram Strait. *A. arcticum* is absent or rare (< 2 % of the assemblage) in sediment dated ∼ 15–12 ka, suggesting minimal perennial sea-ice cover and probably summer sea-ice-free conditions during late deglacial warming.

4.5 The Holocene (∼ 11 to present)

Krithe and *Cytheropteron* remain abundant in sediment dated ∼ 10–7 ka (early Holocene) across most of the central Arctic Basin, signifying continued influence of water derived from the North Atlantic Ocean (Figs. 4, 5). Also during this time, *R. mirabilis* reappears and spikes to an abundance of 55 % at ∼ 8 ka. *A. arcticum* (which represents the *A. arcticum*

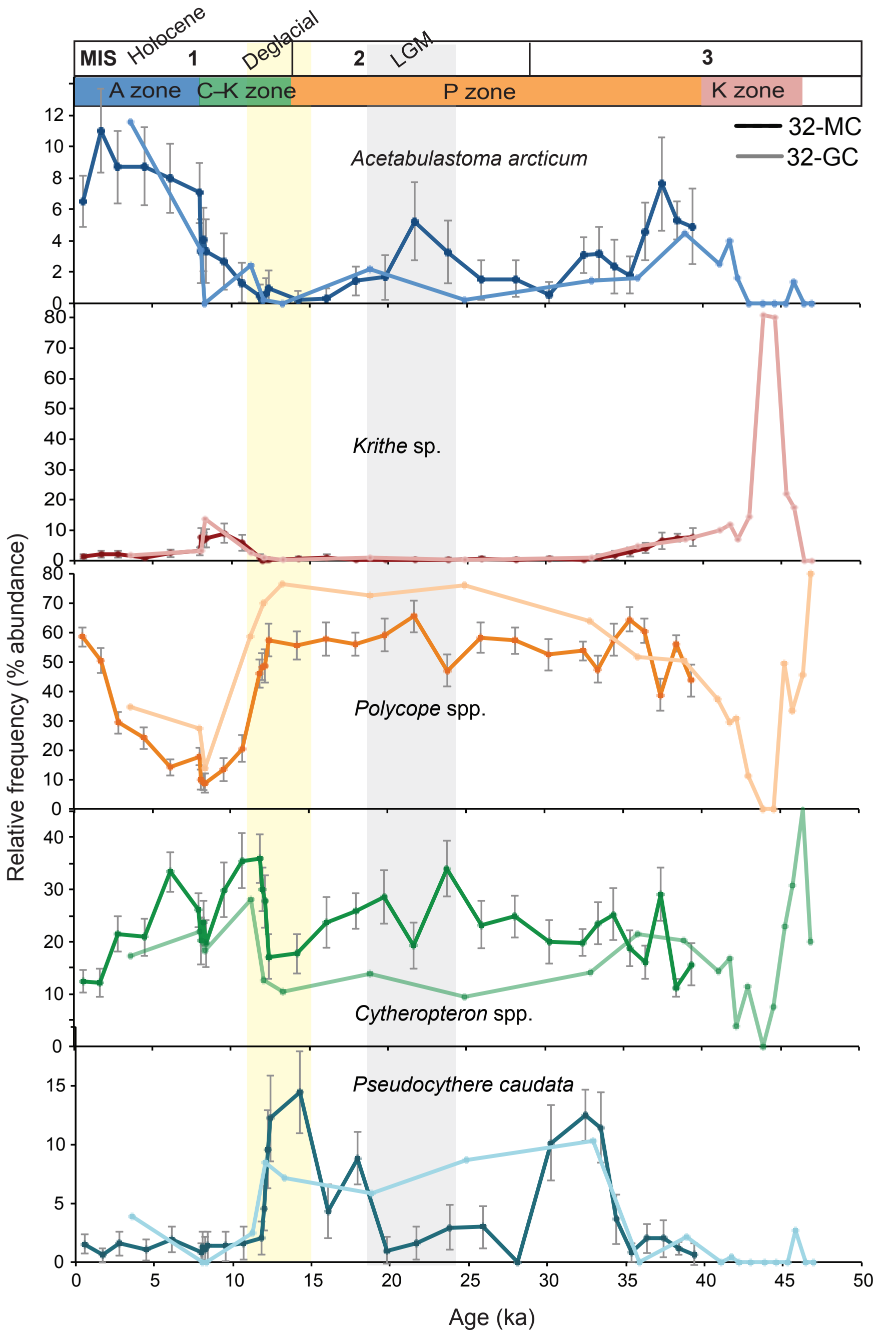

Figure 3. Relative frequencies (percent abundance) of dominant taxa in SWERUS-C3 32-MC and 32-GC. The y axis shows the modeled, mean age during a 2σ range of uncertainty.

zone) increases to > 6–8 % abundance beginning in sediment dated ∼ 7 ka, and increases to > 10 % abundance in sediment dated ∼ 3 ka. This increase in abundance is correlated with an increase in perennial sea ice, and is more prominent in cores from the Lomonosov Ridge than in cores from the Mendeleev Ridge (most likely due to more persistent perennial sea-ice cover over the Lomonosov Ridge sites). The inferred middle to late Holocene development of perennial sea ice is consistent with interpretations from other sea-ice proxies (Xiao et al., 2015) and with the transition from an early–middle Holocene "thermal maximum" (Kaufman et al., 2004, 2016) to cooler conditions during the last few thousand years.

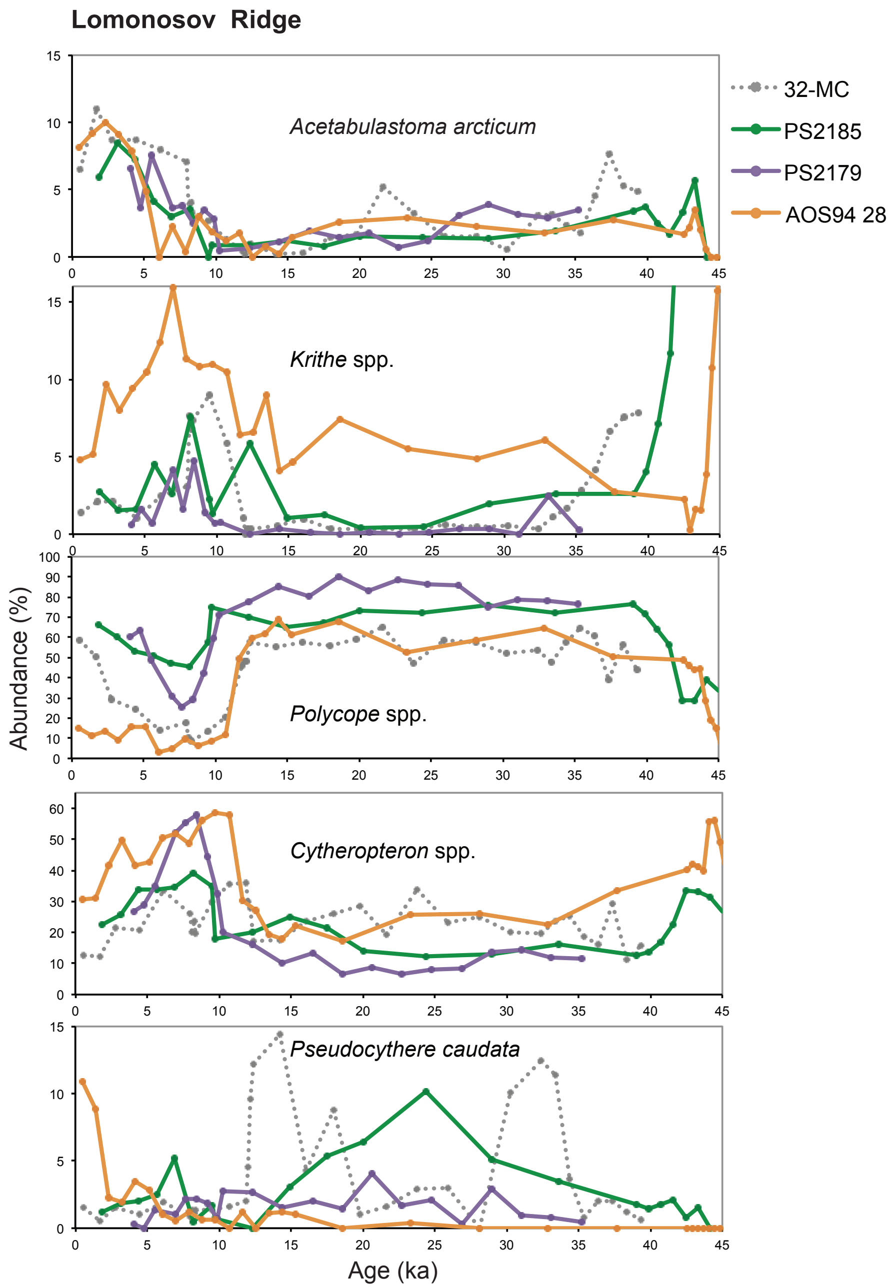

Figure 4. Relative frequencies (percent abundance) of dominant taxa in SWERUS 32-MC (dotted line) compared to other Lomonosov Ridge cores 2185, 2179 and AOS94 28 (Poirier et al., 2012). The chronology for core PS 2185-4 MC (1051 m) is described in Jakobsson et al. (2000), Nørgaard-Pederson et al. (2003), and Spielhagen et al. (2004), core PS 2179-3 MC (1228 m) in Nørgaard-Pederson et al. (2003) and Poirier et al. (2012), and core AOS94 28 (PI-94-AR-BC28, 1990 m) in Darby et al. (1997).

4.6 *Rabilimis mirabilis*: new faunal events signifying rapid oceanographic change

In addition to the standard ostracode zones discussed above, the cores from the SWERUS 2014 expedition provide evidence of uncharacteristic and brief yet significant events of faunal dominance of a taxon. Such events are indicative of rapid environmental change. For example, prior studies have documented range shifts in Arctic benthic foraminifera during the last deglacial and Holocene intervals from the eastern Arctic Ocean (Wollenburg et al., 2001), the Laptev Sea (Taldenkova et al., 2008, 2012), the Beaufort Sea and Amundsen Gulf (Scott et al., 2009) and in older sediments (Polyak et al., 1986, 2004; Ishman and Foley, 1996; Cronin et al., 2014). The SWERUS-32 data reveal two *Rabilimis*

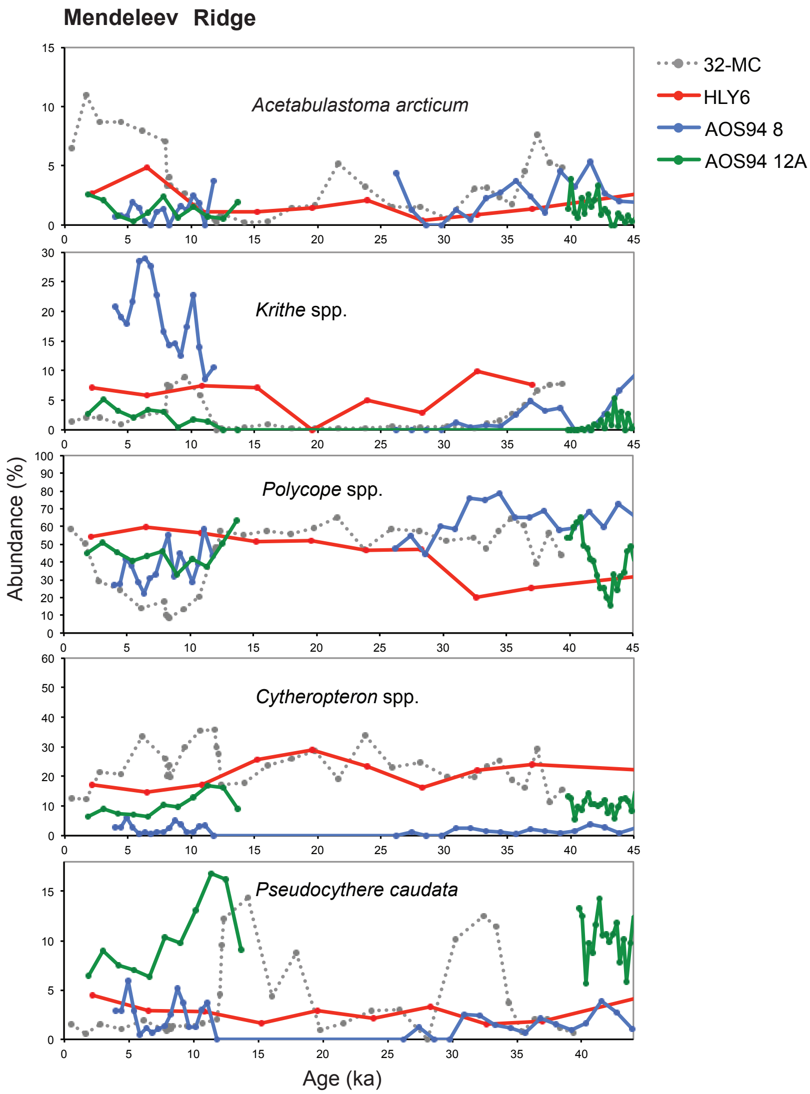

Figure 5. Relative frequencies (percent abundance) of dominant taxa in SWERUS 32-MC (dotted line) compared to other Mendeleev Ridge cores AOS94 8 (Poirier et al., 2012), AOS94 12, and HLY6. The chronology for core HLY6 (HLY0503-06JPC, 800 m) is described in Cronin et al. (2013); core AOS94 8 (PI-94-AR-BC8, 1031 m) in Cronin et al. (2010) and Poirier et al. (2012); and core AOS94 12A (PI-94-AR-BC12A, 1683 m) in Cronin et al. (2010).

Table 5. Although *R. mirabilis* (Brady, 1868) is known and named from Pleistocene sediments in England and Scotland (Brady et al., 1874), this list cites various workers since that have documented this species in Arctic deposits dating back to the late Pliocene, when summer bottom temperatures were inferred to be up to 4 °C warmer than today.

Citation	Location/formation (age)
Siddiqui (1988)	Eastern Beaufort Sea's Iperk sequence (Plio-Pleistocene)
Repenning et al. (1987)	Alaska's North Slope Gubik Formation (Pliocene)
Penney (1990)	Central North Sea deposits (early Pleistocene age, 1.0–0.73 Ma)
Feyling-Hassen (1990)	East Greenland's Kap København Formation (late Pliocene)
Penney (1993)	East Greenland's Lodin Elv Formation (late Pliocene)

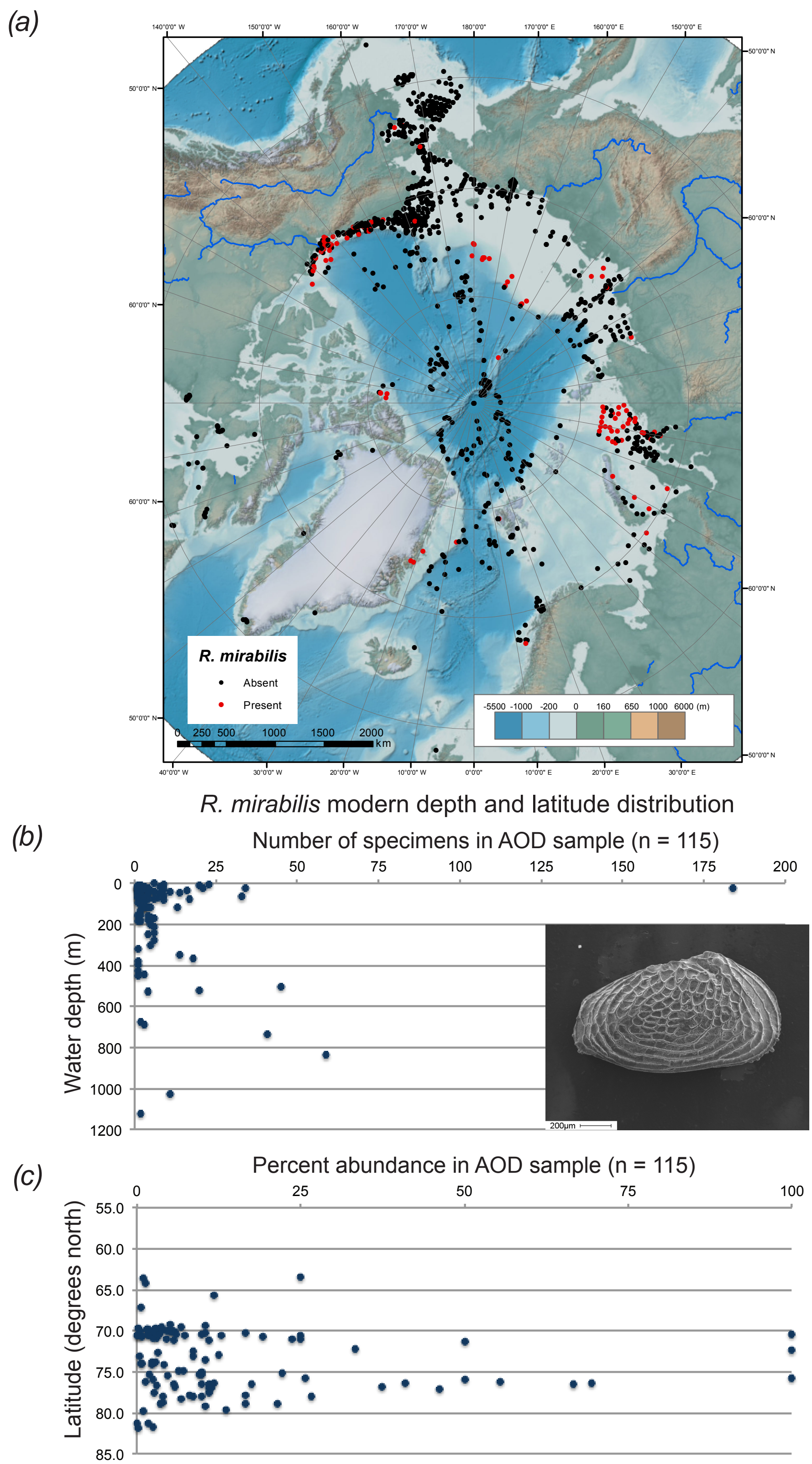

Figure 6. **(a)** Occurrence map of *Rabilimis mirabilis* in the Arctic Ocean and surrounding seas based on 1340 modern surface samples in the Arctic Ostracode Database (AOD; Gemery et al., 2015). **(b)** Modern depth and **(c)** latitudinal distribution of *R. mirabilis* based on 1340 modern surface samples in the AOD (Gemery et al., 2015).

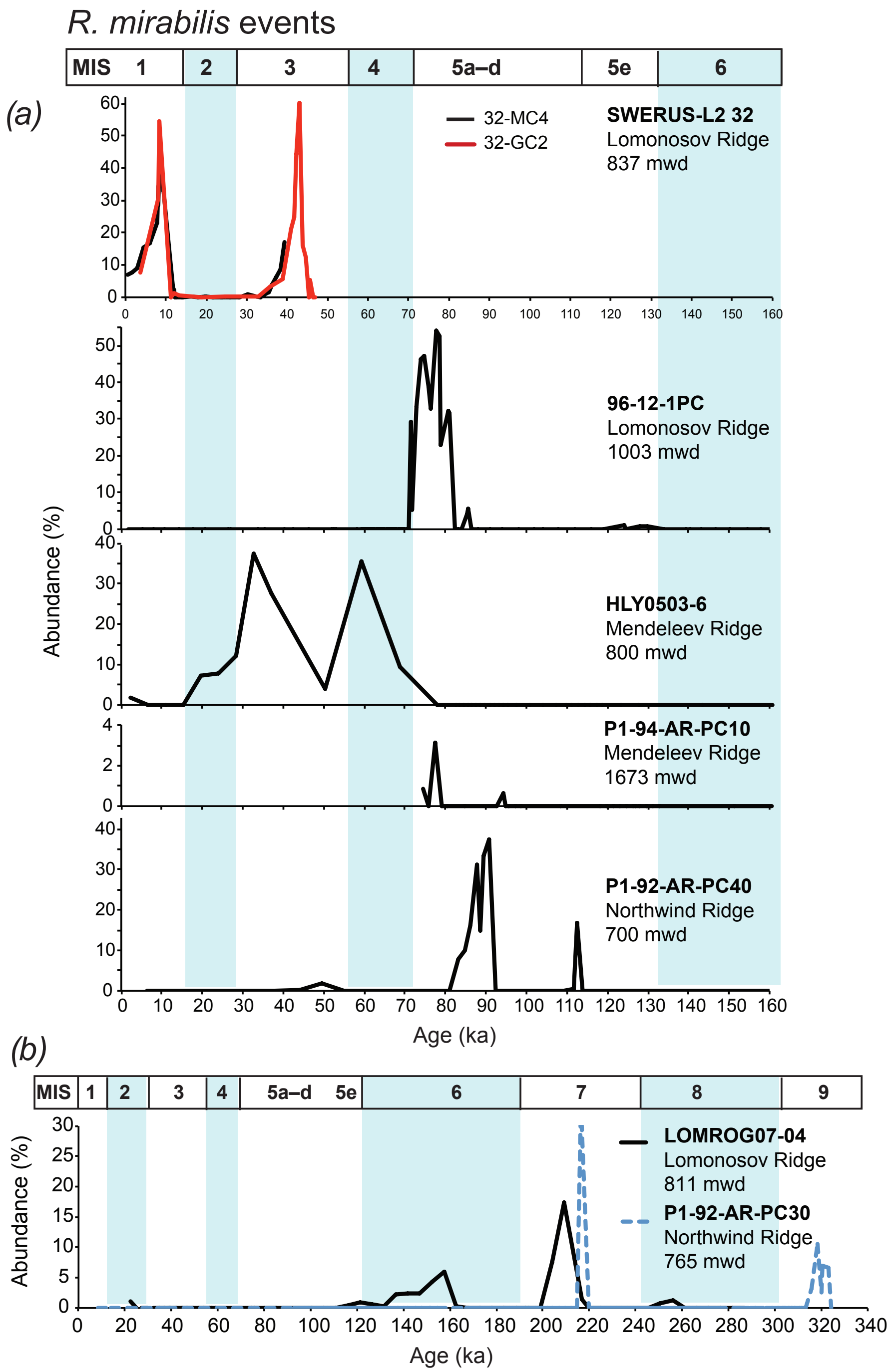

Figure 7. **(a)** Relative frequency (percent abundance) of *R. mirabilis* in SWERUS-32 cores and in central Arctic Ocean cores, 160 ka to present. **(b)** *R. mirabilis* in core LOMROG07-04 from 260 ka to present and in core P1-92-AR-PC30 from 340 ka to present.

mirabilis "events" – intervals containing high proportions of this shallow water ostracode species dated at ~45–36 and 9–8 ka. The modern circum-Arctic distribution of *R. mirabilis* is confined to shallow (< 200 m) water depths (Fig. 6a, b, and c; Hazel, 1970; Neale and Howe, 1975; Taldenkova et al., 2005; Stepanova, 2006; Gemery et al., 2015) and Table 5 lists historical occurrences. *R. mirabilis* can also tolerate a range of salinities, explaining its presence in regions near river mouths with reduced salinity (Fig. 6a). *R. mirabilis* also occurs in 2014 SWERUS-C3 multicore top samples on the eastern Siberian Sea slope (Supplement Table S5; cores 23-MC4 (4 %, 522 m), 18-MC4 (18 %, 349 m), 16-MC4 (11 %, 1023 m), 15-MC4 (41 %, 501 m) and 14-MC4 (70 %, 837 m). These locations correspond to the summer sea-ice edge that has receded during recent decades over the Lomonosov Ridge.

Figure 7a and b show the stratigraphic distribution of *R. mirabilis* at the new SWERUS site and other sites on the Lomonosov Ridge (96-12-1PC), the Mendeleev Ridge (P1-94-AR-PC10) and Northwind Ridge (P1-92-AR-PC40) and in longer cores on the Lomonosov and Northwind Ridge. These patterns suggest a depth range extension of *R. mirabilis* into deeper water (700 to 1673 m) during interstadial periods (MIS 5c, 5a, 3). The abundance of *R. mirabilis* reaches 40–50 % of the total assemblage at Lomonosov Ridge site 96-12-1PC at a water depth of 1003 m. Such anomalously high percentages of well-preserved adult and juvenile specimens of *R. mirabilis* indicate that they were not brought to the site through sediment transport from the shelf. Instead, the *R. mirabilis* events represent in situ populations. Although these *R. mirabilis* events are not synchronous, most occur in sediment dated ∼ 96–71 ka (late MIS 5) and at SWERUS-C3 sites of 32-MC and 32-GC in sediment dated 45–36 and ∼ 9–8 ka (early Holocene). Thus the *R. mirabilis* events correlate with interglacial/interstadial periods that experienced summer sea-ice-free and/or sea-ice edge environments or Atlantic Water inflow. However, additional study of cores from Arctic margins will be required to confirm the paleoceanographic significance of *R. mirabilis* migration events.

5 Conclusions

Changes in ostracode assemblages in new cores from the central Arctic Ocean signify major paleoceanographic shifts at orbital and suborbital scales during the last 50 kyr. Peaks in dominant ostracode taxa include (1) the *Krithe* zone (∼ 45–35 ka), (2) *Polycope* zone (∼ 40–12 ka), (3) *Cytheropteron-Krithe* zone (∼ 12–7 ka), and (4) *Acetabulastoma arcticum* zone (∼ 7 ka–present). Brief yet significant depth migrations of *R. mirabilis* corresponding with the *Krithe* zone and *Cytheropteron–Krithe* zone imply rapid paleoceanographic changes associated with influx of Atlantic Water and/or deep-ocean convection during suborbital events in MIS 3 and the late deglacial to early Holocene. When ostracode assemblage patterns in 32-MC/GC cores are compared to similar records from the Northwind, central Lomonosov, Mendeleev and Gakkel ridges (Cronin et al., 1995, 2010; Poirier et al., 2012), these changes demonstrate pan-Arctic, nearly synchronous changes in benthic ecosystems in association with rapid sea ice, surface productivity, and oceanographic changes in the Atlantic Water and Arctic Intermediate Water during MIS 3–1 (the last 50 kyr). These results confirm the sensitivity of Arctic benthic fauna to large, sometimes abrupt, climate transitions.

Data availability. Additional 2014 SWERUS-C3 expedition data, such as sampling sites, cruise track lines and geophysical mapping profiles, are available through the Bolin Centre for Climate Research database: http://bolin.su.se/data/swerus/ (Bolin Centre for Climate Research, 2017).

The Supplement related to this article is available online at https://doi.org/10.5194/cp-13-1473-2017-supplement.

Competing interests. The authors declare that they have no conflict of interest.

Special issue statement. This article is part of the special issue "Climate-carbon-cryosphere interactions in the East Siberian Arctic Ocean: past, present and future (TC/BG/CP/OS inter-journal SI)". It is not affiliated with a conference.

Acknowledgements. We are grateful to the crew of Icebreaker *Oden* and the SWERUS-C3 Scientific Team. Thanks to Anna Ruefer for assistance with sample processing. This paper benefitted from reviews by Xavier Crosta, Anne de Vernal, Chris Swezey and Michael Toomey. This study was funded by the U.S. Geological Survey Climate R&D Program. Any use of trade, firm, or product names is for descriptive purposes only and does not imply endorsement by the U.S. Government. Andrey Koshurnikov acknowledges financial support from the Russian Government (grant number 14, Z50.31.0012/03.19.2014).

Edited by: Carlo Barbante
Reviewed by: Anne de Vernal, Xavier Crosta, and one anonymous referee

References

Aagaard, K. and Cannack, E. C.: The role of sea ice and other fresh water in the Arctic circulation, J. Geophys. Res., 94, 485–498, https://doi.org/10.1029/JC094iC10p14485, 1989.

Anderson, L. G., Olsson, K., and Skoog, A.: Distribution of dissolved inorganic and organic carbon in the Eurasian Basin of the Arctic Ocean, in: The Polar Oceans and their Role in Shaping the Global Environment, edited by: Johannessen, O. M., Muench, R, D., and Overland, J. E., Geophysical Monograph 85, American Geophysical Union, 525–562, 1994.

Anderson, L. G., Björk, G., Jutterström, S., Pipko, I., Shakhova, N., Semiletov, I., and Wåhlström, I.: East Siberian Sea, an Arctic region of very high biogeochemical activity, Biogeosciences, 8, 1745–1754, https://doi.org/10.5194/bg-8-1745-2011, 2011.

Backman, J., Jakobsson, M., Lovlie, R., Polyak, L., and Febo, L. A.: Is the central Arctic Ocean a sediment starved basin?, Quaternary Sci. Rev., 23, 1435–1454, 2004.

Bolin Centre for Climate Research: Bolin Centre Database, available at: https://bolin.su.se/data/, last access: November 2017.

Brady, G. S.: A Monograph of the Recent British Ostracoda, Transact Linn Soc London, 26, 353–495, 1868.

Brady, G. S., Crosskey, H. W., and Robertson, D.: A Monograph of the Post-Tertiary Entomostraca of Scotland, Including Species from England and Ireland, Paleontograph. Soc. London, 28, 1–232, 1874.

Bronk Ramsey, C.: Bayesian Analysis of Radiocarbon Dates, Radiocarbon, 51, 337–360, https://doi.org/10.2458/azu_js_rc.v51i1.3494, 2009.

Chierici, M. and Fransson, A.: Calcium carbonate saturation in the surface water of the Arctic Ocean: undersaturation in freshwater influenced shelves, Biogeosciences, 6, 2421–2431, https://doi.org/10.5194/bg-6-2421-2009, 2009.

Cronin, T. M., Holtz Jr., T. R., and Whatley, R. C.: Quaternary Paleoceanography of the deep Arctic Ocean based on quantitative analysis of Ostracoda, Mar. Geol., 19, 305–332, https://doi.org/10.1016/0025-3227(94)90188-0, 1994.

Cronin, T. M., Holtz Jr., T. R., Stein, R., Spielhagen, R., Fütterer, D., and Wollenberg, J.: Late Quaternary paleoceanography of the Eurasian Basin, Arctic Ocean, Paleoceanography, 10, 259–281, https://doi.org/10.1029/94PA03149, 1995.

Cronin, T. M., Gemery, L., Briggs Jr., W. M., Jakobsson, M., Polyak, L., and Brouwers, E. M.: Quaternary Sea-ice history in the Arctic Ocean based on a new Ostracode sea-ice proxy, Quaternary Sci. Rev., 1–15, https://doi.org/10.1016/j.quascirev.2010.05.024, 2010.

Cronin, T. M., Dwyer, G. S., Farmer, J., Bauch, H. A., Spielhagen, R. F., Jakobsson, M., Nilsson, J., Briggs, W. M., and Stepanova, A.: Deep Arctic Ocean warming during the Last Glacial cycle, Nat. Geosci., 5, 631–634, 2012.

Cronin, T. M., Polyak L., Reed, D., Kandiano, E. S., Marzen, R. E., and Council, E. A.: A 600-ka Arctic sea-ice record from Mendeleev Ridge based on ostracodes, Quaternary Sci. Rev., 79, 157–167, 2013.

Cronin, T. M., DeNinno, L. H., Polyak, L., Caverly, E. K., Poore, R. Z., Brenner, A., Rodriguez-Lazaro, J., and Marzen, R. E.: Quaternary ostracode and foraminiferal biostratigraphy and paleoceanography in the western Arctic Ocean, Mar. Micropaleontol., 111, 118–133, 2014.

Darby, D. A., Bischof, J. F., and Jones, G. A: Radiocarbon chronology of depositional regimes in the western Arctic Ocean, Deep-Sea Res., 44, 1745–1757, 1997.

Feyling-Hanssen, R. W.: Foraminiferal stratigraphy in the Plio-Pleistocene Kap København Formation, North Greenland, Meddelelser om Grønland, Geoscience, 24, 1–32, 1990.

Gemery, L., Cronin, T. M., Briggs Jr., W. M., Brouwers, E. M., Schornikov, E. I., Stepanova, A., Wood, A. M., and Yasuhara, M.: An Arctic and Subarctic ostracode database: biogeographic and paleoceanographic applications, Hydrobiologia, 1–37, https://doi.org/10.1007/s10750-015-2587-4, 2015.

Grebmeier, J. M.: Shifting Patterns of Life in the Pacific Arctic and Sub-Arctic Seas, Annu. Rev. Mar. Sci., 4, 63–78, 2012.

Grebmeier, J. M. and Barry, J. P.: The influence of oceanographic processes on pelagic-benthic coupling in polar regions: A benthic perspective, J. Mar. Syst., 2, 495–518, 1991.

Grebmeier, J. M., Overland, J. E., Moore, S. E., Farley, E. V., Carmack, E. C., Cooper, L. W., Frey, K. E., Helle, J. H., McLaughlin, F. A., and McNutt, S. L.: A major ecosystem shift in the northern Bering Sea, Science, 311, 1461–1464, https://doi.org/10.1126/science.1121365, 2006.

Hanslik, D., Jakobsson, M., Backman, J., Bjorck, S., Sellen, E., O'Regan, M., Fornaciari, E., and Skog, G.: Quaternary Arctic Ocean sea ice variations and radiocarbon reservoir age corrections, Quaternary Sci. Rev., 29, 3430–3441, 2010.

Hazel, J. E.: Atlantic continental shelf and slope of the United States-ostracode zoogeography in the southern Nova Scotian and northern Virginian faunal provinces, U.S. Geological Survey Professional Paper, 529-E, E1-E21, 1970.

Ishman, S. E. and Foley, K. M.: Modern benthic foraminifer distribution in the Amerasian Basin, Arctic Ocean, Micropaleontology, 42, 206–220, 1996.

Jakobsson, M., Lovlie, R., Arnold, E. M., Backman, J., Polyak, L., Knutsen, J. O., and Musatov, E.: Pleistocene stratigraphy and paleoenvironmental variation from Lomonosov Ridge sediments, central Arctic Ocean, Global Planet. Change, 31, 1–22, 2001.

Jakobsson, M., Nilsson, J., Anderson, L. G., Backman, J., Bjork, G., Cronin, T. M., Kirchner, N., Koshurnikov, A., Mayer, L., Noormets, R., O'Regan, M., Stranne, C., Ananiev, R., Barrientos Macho, N., Cherniykh, D., Coxall, H., Eriksson,B., Floden, T., Gemery, L., Gustafsson, O., Jerram, K., Johansson, C., Khortov, A., Mohammad, R., and Semiletov, I.: Evidence for an ice shelf covering the central Arctic Ocean during the penultimate glaciation, Nat. Comm., 7, 10365, https://doi.org/10.1038/ncomms10365, 2016.

Jakobsson, M., Pearce, C., Cronin, T. M., Backman, J., Anderson, L. G., Barrientos, N., Björk, G., Coxall, H., de Boer, A., Mayer, L. A., Mörth, C.-M., Nilsson, J., Rattray, J. E., Stranne, C., Semiletov, I., and O'Regan, M.: Post-glacial flooding of the Bering Land Bridge dated to 11 cal ka BP based on new geophysical and sediment records, Clim. Past, 13, 991–1005, https://doi.org/10.5194/cp-13-991-2017, 2017.

Jones, E. P.: Circulation in the Arctic Ocean, Polar Res., 20, 139–146, 2001.

Joy, J. A. and Clark, D. L.: The distribution, ecology and systematics of the benthic Ostracoda of the central Arctic Ocean, Micropaleontology, 23, 129–154, 1977.

Karanovic, I. and Brandão, S. N.: Review and phylogeny of the Recent Polycopidae (Ostracoda, Cladocopina), with descriptions of nine new species, one new genus, and one new subgenus from the deep South Atlantic, Mar. Biodivers., 42, 329–393, 2012.

Karanovic, I. and Brandão, S. N.: The genus Polycope (Polycopidae, Ostracoda) in the North Atlantic and Arctic: taxonomy, distribution, and ecology, Syst. Biodivers., 14, 198–223, 2016.

Kaufman, D. S., Ager, T. A., Anderson, N. J., Anderson, P. M., Andrews, J. T., Bartlein, P. J., Brubaker, L. B., Coats, L. L., Cwynar, L. C., Duvall, M. L., Dyke, A. S., Edwards, M. E., Eisner, W. R., Gajewski, K., Geirsdottir, A., Hu, F. S., Jennings, A. E., Kaplan, M. R., Kerwin, M. N., Lozhkin, A. V., MacDonald, G. M., Miller, G. H., Mock, C. J., Oswald, W. W., Otto-Bliesner, B. L., Porinchu, D. F., Ruhland, K., Smol, J. P., Steig, E. J., and Wolfe, B. B.: Holocene thermal maximum in the western Arctic (0–180 degrees W), Quaternary Sci. Rev., 23, 529–560, 2004.

Kaufman, D. S., Axford, Y. L., Henderson, A. C. G., McKay, N. P., Oswald, W. W., Saenger, C., Anderson, R. S., Bailey, H. L., Clegg, B., Gajewski, K., Hu, F. S., Jones, M. C., Massa, C., Routson, C. C., Werner, A., Wooller, M. J., and Yu, Z. C.: Holocene climate changes in eastern Beringia (NW North America) - A systematic review of multi-proxy evidence, Quaternary Sci. Rev., 147, 312–339, 2016.

Laxon, S. W., Giles, K. A., Ridout, A. L., Wingham, D. J., Willatt, R., Cullen, R., Kwok, R., Schweiger, A., Zhang, J., Haas, C., Hendricks, S., Krishfield, R., Kurtz, N., Farrell, S. L., and Davidson, M.: CryoSat estimates of Arctic sea ice volume, Geophys. Res. Lett., 40, 732–737, https://doi.org/10.1002/grl.50193, 2013.

Moore, G. W. K., Våge, K., Pickart, R. S., and Renfrew, I. A.: Decreasing intensity of open-ocean convection in the Greenland and Iceland seas, Nature Climate Change, 5, 877–882, https://doi.org/10.1038/nclimate2688, 2015.

Neale, J. W. and Howe, H. V.: The marine Ostracoda of Russian Harbour, Novaya Zemlya and other high latitude faunas, Bull. Am. Paleontol., 65, 381–431, 1975.

Norgaard-Pedersen, N., Spielhagen, R. F., Thiede, J., and Kassens, H.: Central Arctic surface ocean environment during the past 80,000 years, Paleoceanography, 13, 193–204, https://doi.org/10.1029/97pa03409, 1998.

Nørgaard-Pederson, N., Spielhagen, R. F., Erlenkeuser, H., Grootes, P. M., Heinemeier, J., and Knies, J.: Arctic Ocean during the Last Glacial Maximum: Atlantic and polar domains of surface water mass distribution and ice cover, Paleoceanography, 18, 1063, https://doi.org/10.1029/2002PA000781, 2003.

Nørgaard-Pedersen, N., Mikkelsen, N., Lassen, S. J., Kristoffersen, Y., and Sheldon, E.: Reduced sea ice concentrations in the Arctic Ocean during the last interglacial period revealed by sediment cores off northern Greenland, Paleoceanography, 22, PA1218, https://doi.org/10.1029/2006PA001283, 2007.

Olsson, K. and Anderson, L. G.: Input and biogeochemical transformation of dissolved carbon in the Siberian shelf seas, Cont. Shelf Res., 17, 819–833, 1997.

O'Regan, M.: Late Cenozoic paleoceanography of the central Arctic Ocean, IOP Conf. Series: Earth and Environmental Science 14, https://doi.org/10.1088/1755-1315/14/1/012002, 2011.

Pearce, C., Varhelyi, A., Wastegård, S., Muschitiello, F., Barrientos, N., O'Regan, M., Cronin, T. M., Gemery, L., Semiletov, I., Backman, J., and Jakobsson, M.: The 3.6 ka Aniakchak tephra in the Arctic Ocean: a constraint on the Holocene radiocarbon reservoir age in the Chukchi Sea, Clim. Past, 13, 303–316, https://doi.org/10.5194/cp-13-303-2017, 2017.

Penney, D. N.: Quaternary ostracod chronology of the central North Sea: The record from BH 81/29, Courier Forschungs-Institut Senckenberg, 123, 97–109, 1990.

Penney, D. N.: Late Pliocene to Early Pleistocene ostracod stratigraphy and palaeoclimate of the Lodin Elv and Kap København formations, East Greenland, Palaeogeogr. Palaeoclimatol. Palaeoecol., 101, 49–66, 1993.

Poirier, R. K., Cronin, T. M., Briggs, W. M., and Lockwood, R.: Central Arctic paleoceanography for the last 50 kyr based on ostracode faunal assemblages, Mar. Micropaleontol., 101, 194–194, 2012.

Polyak, L., Curry, W. B., Darby, D. A., Bischof, J., and Cronin, T. M.: Contrasting glacial/interglacial regimes in the western Arctic Ocean as exemplified by a sedimentary record from the Mendeleev Ridge, Palaeogeogr. Palaeocl., 203, 73–93, 2004.

Polyak, L., Bischof, J., Ortiz, J., Darby, D., Channell, J., Xuan, C., Kaufman, D., Lovlie, R., Schneider, D., and Adler, R.: Late Quaternary stratigraphy and sedimentation patterns in the western Arctic Ocean, Global Planet. Change, 68, 5–17, 2009.

Polyak, L., Alley, R. B., Andrews, J. T., Brigham-Grette, J., Darby, D., Dyke, A., Fitzpatrick, J. J., Funder, S., Holland, M., Jennings, A., Miller, G. H., Savelle, J., Serreze, M., White, J. W. C., and Wolff, E.: History of Sea Ice in the Arctic, Quaternary Sci. Rev., 29, 1757–1778, 2010.

Polyak, L. V.: New data on microfauna and stratigraphy of bottom sediments of the Mendeleev Ridge, Arctic Ocean, in: Sedimentogenes i konkrecioobrazovanie v okeane (Sedimentogenesis and nodule-formation in the Ocean), edited by: Andreev, S. I., Sevmorgeologia, Leningrad, 40–50, 1986 (in Russian).

Polyakov, I. V., Pnyushkov, A. V., Alkire, M. B., Ashik, I. M., Baumann, T. M., Carmack, E. C., Goszczko, I., Guthrie, J., Ivanov, V. V., Kanzow, T., Krishfield, R., Kwok, R., Sundfjord, A., Morison, J., Rember, R., and Yulin, A.: Greater role for Atlantic inflows on sea-ice loss in the Eurasian Basin of the Arctic Ocean, Science, 356, 285–291, https://doi.org/10.1126/science.aai8204, 2017.

Rabe, B., Karcher, M., Schauer, U., Toole, J. M., Krishfield, R. A., Pisarev, S., Kauker, F., Gerdes, R., and Kikuchi, T.: An assessment of Arctic Ocean freshwater content changes from the 1990s to the 2006–2008 period, Deep Sea Res. Pt I, 58, 173, https://doi.org/10.1016/j.dsr.2010.12.002, 2011.

Raup, D. M.: The future of analytical paleobiology, in: Analytical Paleobiology: Paleontological Society Short Courses in Paleontology, edited by: Gilinsky, N. L. and Signor, P. W., 4, 207–216, 1991.

Reimer, P. J. and Reimer, R. W.: A marine reservoir correction database and on-line interface, Radiocarbon, 43, 461–463, 2001.

Reimer, P. J., Bard, E., Bayliss, A., Beck, J. W., Blackwell, P. G., Bronk Ramsey, C., Grootes, P. M., Guilderson, T. P., Haflidason, H., Hajdas, I., Hatté, C., Heaton, T. J., Hoffmann, D. L., Hogg, A. G., Hughen, K. A., Kaiser, K. F., Kromer, B., Manning, S. W., Niu, M., Reimer, R. W., Richards, D. A., Scott, E. M., Southon, J. R., Staff, R. A., Turney, C. S. M., and van der Plicht, J.: IntCal13 and Marine13 Radiocarbon Age Calibration Curves 0–50,000 Years cal BP, Radiocarbon, 55, 1869–1887, https://doi.org/10.2458/azu_js_rc.55.16947, 2013.

Repenning, C. A., Brouwers, E. M., Carter, L. D., Marincovich Jr., L., and Ager, T. A.: The Beringian ancestry of Phenacomys (Rodentia: Cricetidae) and the beginning of the modern Arctic Ocean Borderland biota, U.S. Geological Survey Bulletin, 1687, 1–31, 1987.

Rigor, I. G., Wallace, J. M., and Colony, R. L.: Response of sea ice to the Arctic oscillation, J. Climate, 15, 2648–2663, 2002.

Rudels, B.: Arctic Ocean circulation and variability – advection and external forcing encounter constraints and local processes, Ocean Sci., 8, 261–286, https://doi.org/10.5194/os-8-261-2012, 2012.

Rudels, B., Schauer, U., Björk, G., Korhonen, M., Pisarev, S., Rabe, B., and Wisotzki, A.: Observations of water masses and circulation with focus on the Eurasian Basin of the Arctic Ocean from the 1990s to the late 2000s, Ocean Sci., 9, 147–169, https://doi.org/10.5194/os-9-147-2013, 2013.

Schornikov, E. I.: Acetabulastoma – a new genus of ostracodes, ectoparasites of Amphipoda, Zoologichesky Zhurnal, 49, 132–1143, 1970 (in Russian).

Scott, D. B., Schell, T., St-Onge, G., Rochon, A., and Blasco, S.: Foraminiferal assemblage changes over the last 15,000 years on the Mackenzie-Beaufort Sea Slope and Amundsen Gulf, Canada: Implications for past sea ice conditions, Paleoceanography, 24, Pa2219, https://doi.org/10.1029/2007pa001575, 2009.

Serreze, M. C. and Stroeve, J.: Arctic sea ice trends, variability and implications for seasonal ice forecasting, Philosophical transactions Series A, Mathematical, physical, and engineering sciences, 373, 20140159, https://doi.org/10.1098/rsta.2014.0159, 2015.

Siddiqui, Q. A.: The Iperk Sequence (Plio-Pleistocene) and its Ostracod Assemblages in the Eastern Beaufort Sea, in: Evolutionary Biology on Ostracoda, edited by: Hanai, T., Ikeya, N., and Ishizaki, K. , Proc. Ninth Int Symp Ostracoda, Kodansha, Tokyo, 533–540, 1988.

Smedsrud, L. H., Halvorsen, M. H., Stroeve, J. C., Zhang, R., and Kloster, K.: Fram Strait sea ice export variability and September Arctic sea ice extent over the last 80 years, The Cryosphere, 11, 65–79, https://doi.org/10.5194/tc-11-65-2017, 2017.

Somavilla, R., Schauer, U., and Budeus, G.: Increasing amount of Arctic Ocean deep waters in the Greenland Sea, Geophys. Res. Lett., 40, 4361–4366, 2013.

Spielhagen, R. F., Baumann, K. H., Erlenkeuser, H., Nowaczyk, N. R., Norgaard-Pedersen, N., Vogt, C., and Weiel, D.: Arctic Ocean deep-sea record of northern Eurasian ice sheet history, Quaternary Sci. Rev., 23, 1455–1483, 2004.

Stein, R., Nam, S. I., Schubert, C., Vogt, C., Fütterer, D., and Heinemeier, J.: The last deglaciation event in the eastern central Arctic Ocean, Science, 264, 692–696, 1994.

Stein, R., Fahl, K., and Müller, J.: Proxy reconstruction of Arctic Ocean sea ice history – From IRD to IP25, Polarforschung, 82, 37–71, 2012.

Stein, R., Fahl, K., Schade, I., Manerung, A., Wassmuth, S., Niessen, F., and Nam, S.-I.: Holocene variability in sea ice cover, primary production, and Pacific-Water inflow and climate change in the Chukchi and East Siberian Seas (Arctic Ocean), J. Quaternary Sci., 32, 362–379, https://doi.org/10.1002/jqs.2929, 2017.

Stepanova, A., Taldenkova, E., and Bauch, H. A.: Recent Ostracoda of the Laptev Sea (Arctic Siberia): taxonomic composition and some environmental implications, Mar. Micropaleontol., 48, 23–48, 2003.

Stepanova, A. Y.: Late Pleistocene-Holocene and Recent Ostracoda of the Laptev Sea and their importance for paleoenvironmental reconstructions, Paleontol. J., 40, S91–S204, 2006.

Stepanova, A., Taldenkova, E., Simstich, J., and Bauch, H. A.: Comparison study of the modern ostracod associations in the Kara and Laptev seas: Ecological aspects, Mar. Micropaleontol., 63, 111–142, 2007.

Stepanova, A. Y., Taldenkova, E. E., and Bauch, H. A.: Arctic quaternary ostracods and their use in paleoreconstructions, Paleontol. J., 44, 41–48, 2010.

Stepanova, A., Taldenkova, E., and Bauch, H. A.: Late Saalian–Eemian ostracods from the northern White Sea region, Joannea Geol Paläont, 11, 196–198 (abstract only), 2011.

Stroeve, J. C., Serreze, M. C., Holland, M. M., Kay, J. E., Malanik, J., and Barrett, A. P.: The Arctic's rapidly shrinking sea ice cover: a research synthesis, Climatic Change, 110, 1005–1027, 2012.

Stroeve, J. C., Markus, T., Boisvert, L., Miller, J., and Barrett, A.: Changes in Arctic melt season and implications for sea ice loss, Geophys. Res. Lett., 41, 2013GL058951, https://doi.org/10.1002/2013GL058951, 2014.

SWERUS C3 2014 Expedition. The Swedish – Russian – US Arctic Ocean Investigation of Climate-Cryosphere-Carbon Interactions – The SWERUS-C3 2014 Expedition Cruise Report Leg 2 (of 2), available at: ftp://ftp.geo.su.se/martinj/outgoing/SWERUSC3/Leg2CruiseReport/, last access: 2016.

Taldenkova, E., Bauch, H. A., Stepanova, A., Dem'yankov, S., and Ovsepyan, A.: Last postglacial environmental evolution of the Laptev Sea shelf as reflected in molluscan, ostracodal, and foraminiferal faunas, Global Planet. Change, 48, 223–251, 2005.

Taldenkova, E., Bauch, H. A., Stepanova, A., Strezh, A., Dem'yankov, S., and Ovsepyan, Y.: Postglacial to Holocene benthic assemblages from the Laptev Sea: paleoenvironmental implications, Quaternary Int., 183, 40–60, 2008.

Taldenkova, E., Bauch, H. A., Stepanova, A., Ovsepyan, Y., Pogodina, I., Klyuvitkina, T., and Nikolaev, S.: Benthic and planktic community changes at the North Siberian margin in response to Atlantic water mass variability since last deglacial times, Mar. Micropaleontol., 96–97, 13–28, https://doi.org/10.1016/j.marmicro.2012.06.007, 2012.

Wassmann, P., Duarte, C. M., Agusti, S., and Sejr, M. K.: Footprints of climate change in the Arctic marine ecosystem, Glob. Change Biol., 17, 1235–1249, 2011.

Whatley, R. C., Eynon, M. P., and Moguilevsky, A.: Recent Ostracoda of the Scoresby Sund Fjord system, East Greenland, Revista Española de Micropaleontologia, 28, 5–23, 1996.

Whatley, R., Eynon, M., and Moguilevsky, A.: The depth distribution of Ostracoda from the Greenland Sea, J. Micropalaeontol., 17, 15–32, 1998.

Wollenburg, J. E., Kuhnt, W., and Mackensen, A.: Changes in Arctic Ocean paleoproductivity and hydrography during the last 145 kyr: The benthic foraminiferal record, Paleoceanography, 16, 65–77, 2001.

Xiao, X., Stein, R., and Fahl, K.: MIS 3 to MIS 1 temporal and LGM spatial variability in Arctic Ocean sea ice cover: Reconstruction from biomarkers, Paleoceanography, 30, 969–983, https://doi.org/10.1002/2015PA002814, 2015.

Yasuhara, M., Stepanova, A., Okahashi, H., Cronin, T. M., and Brouwers, E. M.: Taxonomic revision of deep-sea Ostracoda from the Arctic Ocean, Micropaleontology, 60, 399–444, 2014.

Zarikian, C. A. A., Stepanova, A. Y., and Grutzner, J.: Glacial-interglacial variability in deep sea ostracod assemblage composition at IODP Site U1314 in the subpolar North Atlantic, Mar. Geol., 258, 69–87, 2009.